Article ID: 1000-324X(2017)09-0997-07 **DOI:** 10.15541/jim20170001

Low-cost Preparation of Graphene Papers from Chemical Reduction with FeI_2/Ni^{2+} for Conductivity and Catalytic Property

NAN Hui[1], WANG Wen-Li[2], HAN Jian-Hua[1], YIN Xue-Wen[1], ZHOU Yu[1], ZHAO Xiao-Chong[3], LIN Hong[1]

(1. State Key Laboratory of New Ceramics & Fine Processing, School of Materials Science and Engineering, Tsinghua University, Beijing 100084, China; 2. National Engineering Laboratory for Modern Silk; College of Textile and Clothing Engineering, Soochow University, Suzhou 215123, China; 3. Institute of Materials, China Academy of Engineering Physics, Mianyang 621907, China)

Abstract: A novel method to produce reductive graphene oxide (RGO) with FeI_2/Ni^{2+} applied as reductive agent was reported. This method provides a cheap, effective and environmentally friendly route for the large-scale production of RGO without losing its high conductivity and catalytic activity. An extremely high conductivity of 30231 S/m was obtained affer the optimized $FeI_2/Ni(NO_3)_2$ solution treatment. The enhancement of bulk conductivity was clue to the promotion of the nucleophilic substitution reaction induced by Fe^{2+} (a strong Lewis acid). Ni^{2+} was introduced to optimize the reductive process by reducing the concentration of hydrogen ions, which would inhibit the hydrolysis of Fe^{2+}. Furthermore, a high cathodic peak current density was observed when applying the free-standing RGO paper as counter electrode in I^-/I^{3-} electrolyte system, indicating the high catalytic performance of the RGO paper and providing electron transporting pathway. These outstanding features exhibit a promising prospect of application in solar cells.

Key words: graphene oxide; metal iodides; chemical reduction; bulk conductivity ; catalytic

As a two-dimensional (2D) carbon material, graphene has attracted great attention[1–6] due to its excellent electrical conductivity and mechanical property. Therefore, the graphene has been widely applied in numerous fields, like electronic, optoelectronic and hydrogen storage[7–10]. Compared to the other electronic materials, graphene has been proved to be suitable for the demand of future commercial applications with excellent conductivity and catalytic properties[11].

To date, the production of high conductive single or few-layers graphene has been developed by many methods, such as micro mechanical exfoliation, chemical vapor disposition, and chemical reduction[12-15]. Among all those methods, chemical reduction is widely regarded as a low-cost technique for the prospect of large scale production[16]. In the past few years, plentiful reducing agents such as hydrazine derivate, hydrazine, alcohols, $NaBH_4$, and sodium hydrideand hydroiodic acid[17-22] have been used to reduce graphene oxide (GO). The bulk conductivity of reduced graphene oxide (RGO) papers has been gradually improved. So far, the highest electrical conductivity of 29800 S/m for RGO papers have been obtained by submerging GO papers into 55% HI solution for 1 h at 100℃[23]. However, the relative high cost and strong corrosion property of H^+ limits its further application. A cheap, effective and environmentally friendly method should be further developed to obtain high conductive RGO. Recently, RGO papers with a high electrical conductivity of 19800 S/m have been obtained through submerging GO papers into FeI_2 solution with a pH of 1.5 at 95℃ for 6 h by Lin, *et al*[24]. Metal cation Fe^{2+}, as a strong Lewis acid, can promote the nucleophilic substitution reaction. Meanwhile, FeI_2 solution provides a mild and environmentally benign reductive process.

Another issue hindering the application of RGO in electronic sensor and solar cell field is the difficulty in achieving high conductivity and catalytic property consistently. The catalytic property of RGO is widely improved by the functional groups, which will oppositely decrease the conductivity. It was reported that high catalytic RGO papers could be obtained through submerging GO papers into AlI_3 solution by Lin, *et al*[16]. Nevertheless, the low electrical conductivity of 5320 S/m limited its further application. Therefore, a balance between conductivity and catalytic property should be established.

Herein, a low-cost, green and facile synthetic route for

Received date: 2017-01-03; **Modified date:** 2017-03-20
Foundation item: Ministry of Science & Technology of China: Sino-Italy International Cooperation on Innovation (2016YFE0104000); International Cooperation and Exchanges (NSFC, 51561145007); National Energy Novel Materials Center (NENMC-Ⅱ-1705)
Biography: NAN Hui(1984–), male, candidate of PhD. E-mail: 865615800@qq.com
Corresponding author: LIN Hong, professor. E-mail: hong-lin@mail.tsinghua.edu.cn

highly efficient reduction of GO papers was reported. The obtained free standing RGO film behaves both high conductivity and catalytic property. In the present study, Ni^{2+} solution was introduced to reduce the concentration of hydrogen ions, which would improve the reductive ability by inhibiting the hydrolysis of those strong Lewis acids. The effects of reaction time and temperature on the conductivity of RGO papers accompanied with the different kinds of nickel salt were systematically investigated. In addition, the catalytic activity of RGO papers films for I^-/I_3^- solution was also studied by the cyclic voltammetry measurement.

1 Experimental section

1.1 Reduction of GO to RGO with FeI_2/Ni^{2+}

GO suspension was prepared using a modified Hummers and Offeman's method from natural graphite[24]. To obtain single-layer GO, a low-speed centrifugation (4000 r/min, 5 min) was used to remove thick multilayer flakes and all the visible particles. Then the obtained single-layer GO aqueous supernatant was filtered at vacuum to prepare GO paper on mixed cellulose ester filter membrane. After dried at room temperature for 12 h to remove the remaining solution, the GO paper was immersed into acetone to dissolve the mixed cellulose ester filter membrane and to obtain GO paper.

FeI_2 was synthesized directly from the reaction of I_2 and Fe powder with water as a catalyzer. Different precursor solutions of Ni^{2+}, NO_3^-, Cl^- and SO_4^{2-} were introduced to FeI_2 solution for inhibiting the hydrolysis of Lewis acids. The detailed experimental procedure is described as follow: 2 g I_2 powders were ground into powder in an agate mortar and mixed with 2 g Fe particles in a beaker. Soon after that, the reaction between I_2 and Fe fiercely started and ended in 15 s. Then, the deionized water (200 mL) was added into the beaker, which was stirred until the metal iodide was dissolved. After that, 1.2 mmol/L Ni^{2+} was added into the FeI_2 solution. The mixture solution was decanted into another beaker. Finally, the free-standing GO papers were immersed into the mixture solution to obtain RGO papers. Five GO samples were reduced at each condition to ensure the reproducibility and standard deviation of conductivity was obtained.

1.2 Characterization

To get reliable electrical conductivity data, four different sites of each RGO paper (2 cm×2 cm in size) dried at room temperature in air for 12 h were detected by the four-point probe system (SX1934, Suzhou, China). The thickness of the RGO paper was measured by a scanning electron microscope (SEM, LEO 1530, Gemini, Zeiss, Germany) and TEM (Tecnai F20 TEM, FEI, USA). Raman spectroscopy was performed on a laser micro-Raman spectroscope (Hr 800, Horiba JobinYvon, France) with a laser beam wavelength of 633 nm. The existing functional groups of each sample were measured by a Fourier-transform infrared spectrometer (FTIR, NICOLET560, Nicolet, USA). Composition identification of the samples were performed by the X-ray photoelectron spectroscopy (XPS) spectra (ESCALAB 250 Xi, Thermo SCIENTIFIC, USA) with Al Kα radiation ($h\nu$=1486.6 eV) as source. Crystalline properties of the samples were analyzed by an X-ray diffractometer (XRD, D8 advance, Bruker, Germany). Cyclic voltammetry (CV) was observed in a conventional three-electrode system in acetonitrile solution containing LiI (10 mmol/L), I_2 (1 mmol/L) and 0.1 mol/L $LiClO_4$ (0.1 mol/L) as supporting electrolyte, RGO film or Pt electrode as the counter electrode, Pt foil as a working electrode and Ag/AgCl as a reference electrode using a CHI650C electrochemical analyzer (CH Instrument Corp, 124 USA).

2 Results and discussion

2.1 Electrical conductivity of RGO

The thicknesse of the RGOs was about 2.1 μm (Fig. 1(a)), fairly close to that of original GO film (Fig. 1(b)). As shown in Fig. 1(c), a large-scale free-standing RGO paper with a diameter of 40 mm was produced with robust and highly flexible nature. This is attributed to the high mechanical intensity of flexible GO film. The excellent overlapping properties among these single layer GO flakes could provide strong resistance to avoid expansion or shrinkage. Figure 1(d) and f exhibit the sheet resistance and electrical conductivity of RGO reduced by $FeI_2/Ni(NO_3)_2$ at different time and temperatures. The electrical conductivity increases continuously with temperature increasing from 80℃ to 95℃ (the boiling point of solution). Meanwhile, the RGO film exhibited the highest electrical conductivity of 27000 S/m at the reaction time of 6 h. The XRD patterns of RGO reduced by $FeI_2/Ni(NO_3)_2$ as a function of different temperature (Fig. 2(b)) and time (Fig. 2(c)) was presented. It could be found that the RGO reduced by $FeI_2/Ni(NO_3)_2$ at 95℃ for 6 h showed a higher peak than those of other RGOs, indicating a higher crystallinity of RGO at this condition. Therefore, it seems that crystallinity is decisive for conductivity of RGO. Figure 1(f) shows the sheet resistance and conductivity of RGO reduced by different reductant. Considering that the stability of $Ni(NO_3)_2$ is lower than those of other reagents (ΔG ($NiCl_2$) =–216.856 kJ/mol, ΔG ($Ni(NO_3)_2$) = –176.9 kJ/mol, ΔG ($NiSO_4$) =–698.93 kJ/mol), the weaker

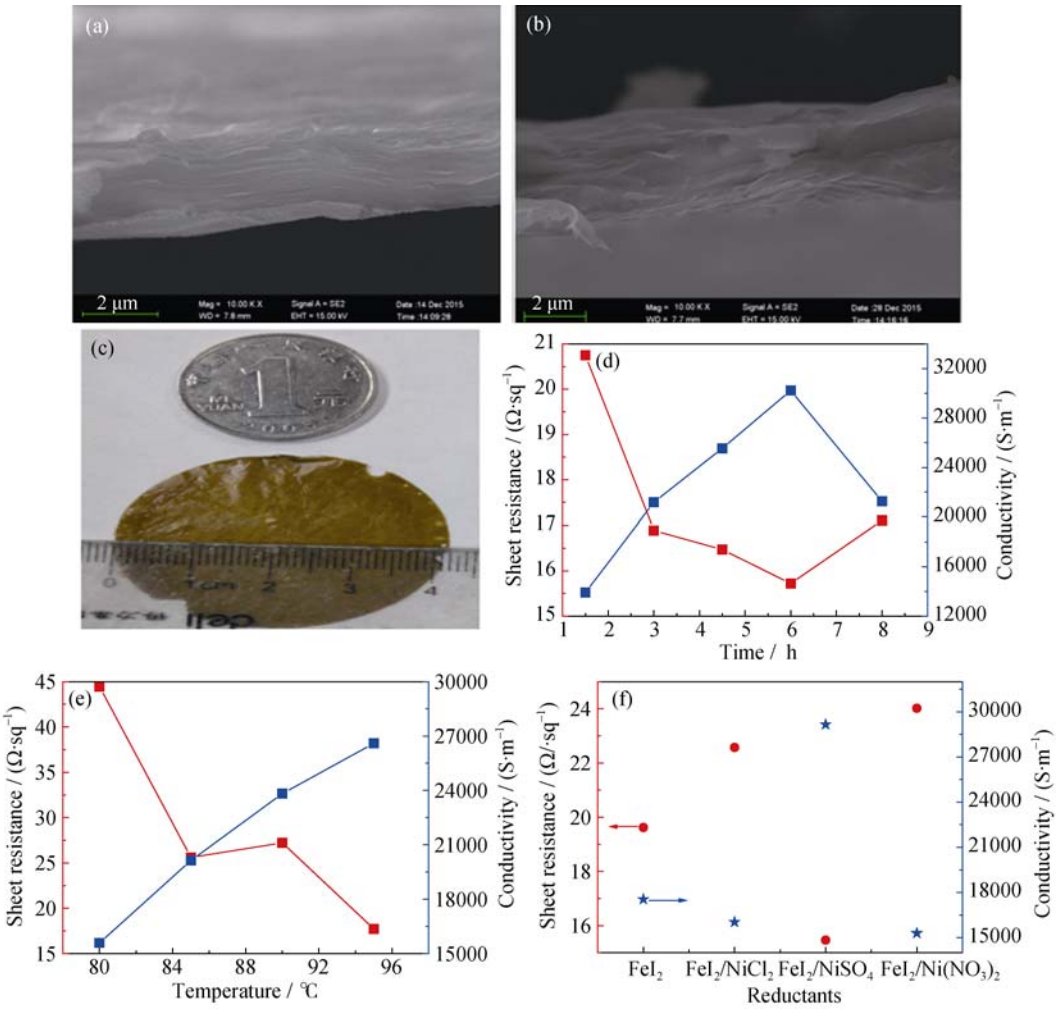

Fig. 1　Cross section SEM images of the original GO film (a) and RGO films (b) after reduction; Sheet resistance and conductivity of as-prepared RGO (c) reduced with different time (d), temperature (e), reductant (f)

attraction of NO_3^- to Ni^{2+} would result in a stronger interaction between Ni^{2+} and Fe^{2+}. Therefore, $Ni(NO_3)_2$ is preferably chosen to suppress Fe^{2+} hydrolyzing to the precipitation of $Fe(OH)_3$ compared with others reductant. What's more, an extremely high bulk conductivity of 30231 S/m (sheet resistance is 15.72 Ω/sq) was obtained, which is higher than the reported highest value of 29800 S/m by 55% HI solution[23].

2.2　Characterization of RGO

Figure 2 showed the XRD patterns of raw graphite, GO, and RGO reduced with different reductant. The sharp peaks at 26.38º and 11.98º attributed to graphite and GO respectively disappeared after reduction with different reductants. Meanwhile, the sharp peak at 23.90º belonging to RGO indicated the transformation from GO to RGO was completed. The crystalline peak of $FeI_2/Ni(NO_3)_2$ reduced RGO was the highest compared with others, implying the enhanced crystallinity of RGO. Better crystallinity would lead to higher bulk conductivity and lower sheet resistance of the $FeI_2/Ni(NO_3)_2$ reduced RGO than those of others.

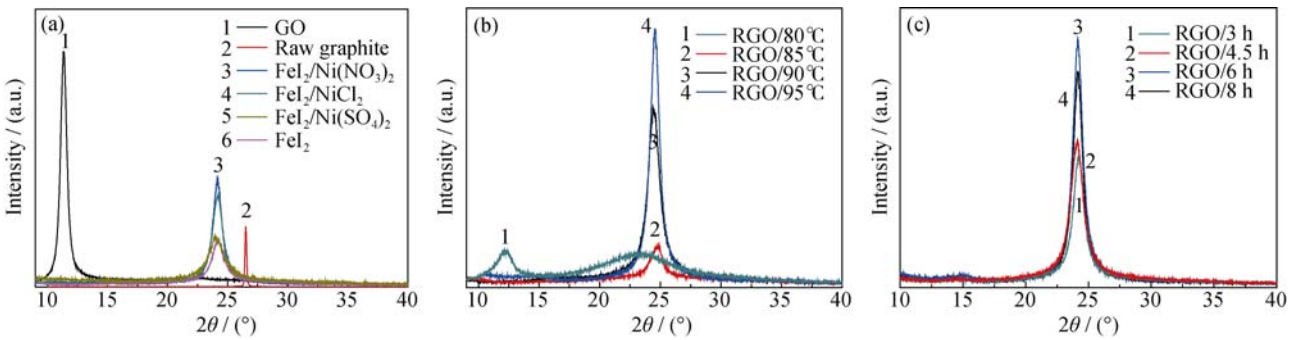

Fig. 2　XRD patterns of raw graphite, GO, and RGO reduced with different reductant (a); by $FeI_2/Ni(NO_3)_2$ with different temperatures (b) and for different time (c)

Figure 3(a) showed the FTIR spectra of GO and RGO reduced with different reductants. The characteristic peaks of GO, including C=O stretching at 1720 cm^{-1}, C–C stretching at 1560 cm^{-1}, C–OH deformation at 1400 cm^{-1}, C–O (epoxy) stretching at 1220 cm^{-1}, and C–O deformation at 1030 and 1060 cm^{-1}, were observed in the FTIR spectrum of GO[25]. For the RGO, the deformed C–C stretching vibration at 1560 cm^{-1} is due to the presence of the neighboring epoxy groups[26], and the intensity of peaks at 1720, 1220, 1060, and 1030 cm^{-1} (corresponding oxygen functional groups) strongly decrease under different reduction solutions. Nevertheless, the elimination of these bands is not complete, indicating that the carbon oxygen groups still exist after the reduction process. Meanwhile, the persistence of the band at about 1400 cm^{-1} (carboxyl C–O) implies that a small number of hydroxyl groups remain in the RGO papers. All the above FTIR results suggest that most of the oxygen functional groups can be removed, however, the hydroxyl group is relatively difficult to be removed. Figure 3(b) shows the Raman spectra of GO and RGO treated with different solutions. It can be found that the D peak intensity of GO is similar to that of G peak intensity, while the D peak intensity of RGO is generally higher than G peak intensity (See detailed I_D/I_G data in Table 1). Large value of I_D/I_G usually indicates low concentration of defects[27]. It can also be found that the defects can be effectively fixed during the GO reduction to RGO with different reductants. Furthermore, the addition of Ni^{2+} leads to higher I_D/I_G, which implies that the presence of Ni^{2+} can inhibit hydrolysis of these strong Lewis acid (Fe^{2+}) further to promote the nucleophilic substitution reaction of oxygen-containing groups, finally to reduce the concentration of defects. Interestingly, the RGO reduced by $FeI_2/Ni(NO_3)_2$ acquires the larger I_D/I_G than those of other RGOs, indicating that the RGO has the lowest defects, leading to the best crystallinity , which is consistent with the XRD results.

Figure 4 shows SEM images of GO (a, b) and TEM images of RGO (c, d) reduced by $FeI_2/Ni(NO_3)_2$. The surface of RGO showed more surface folds compared with that of GO, implying that the oxygen functional group of GO was removed, leading to folded and imbricated structure.

The deconvolution of carbon 1s peaks in XPS patterns of the RGO papers reduced by different reductant (Fig. 5) showed the same results as FTIR spectra: The C–O–C (286.9 eV) and C=O (287.9 eV) peak, which are the major oxygen functional groups (Fig. 5(a)), decreases significantly after reduced with different reductant (Fig. 5(b) and 5(c)). Meanwhile, the C–C peak (284.8 eV) became sharper after reduction, which is consistent with the FTIR results as shown in Fig. 3(a)[28]. The increase of C–C and the decrease of C=O in the XPS spectra lead to the improvement of the performance of electrical conductivity of RGO. However, the carbon oxygen groups are difficult to remove, which prevents the further improvement of the electrical conductivity of RGO. Considering the instability of Fe^{2+} in aqueous solution, $Ni(NO_3)_2$ was introduced to suppress the process of Fe^{2+} hydrolyzing to precipitation of $Fe(OH)_3$, which resulted in the sharper C–C peak at 284.8 eV (Fig. 5(c)) than that reduced by FeI_2 (Fig. 5(b)). Therefore, the RGO reduced by $FeI_2/Ni(NO_3)_2$ has better electrical conductivity than that reduced by FeI_2.

Table 1 I_D/I_G of GO and RGO reduced with different solutions

Sample	Reductant	I_D/(a.u.)	I_G/(a.u.)	I_D/I_G
GO		499.7	462.5	1.08
RGO	FeI_2	377.3	237.3	1.59
RGO	$FeI_2/NiCl_2$	402.2	251.7	1.60
RGO	$FeI_2/Ni(NO_3)_2$	389.6	250.2	1.66
RGO	$FeI_2/NiSO_4$	564.8	389.2	1.45

Figure 6 shows the time-depended color changes of different reductant. Firstly, Fe^{2+} (light green) slowly changed to Fe^{3+} (yellow) with time increasing, implying that Fe^{2+} has been oxidized to Fe^{3+}. Secondly, for $FeI_2/Ni(NO_3)_2$ solutions, the light green change was slower than that of FeI_2 solutions, This indicates that $Ni(NO_3)_2$ can inhibit the hydrolysis of Lewis acids (Fe^{2+}). According to equation (1) and (2), the reaction would proceed because of the strong oxidability of

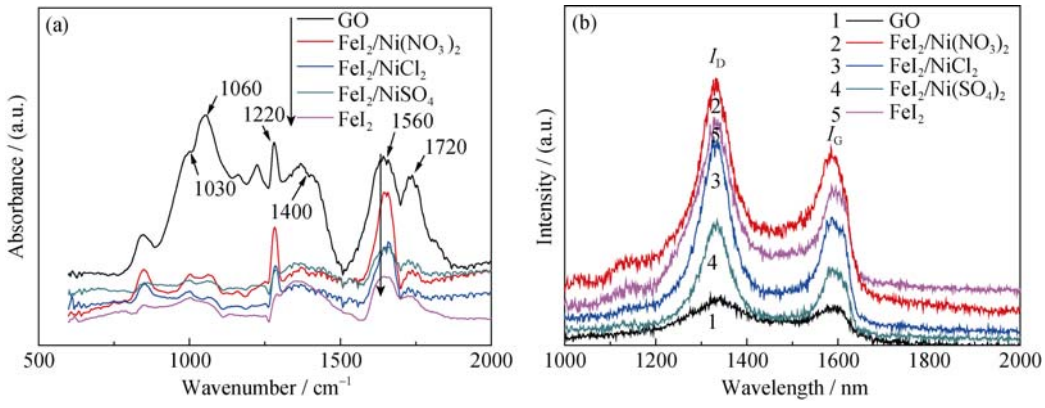

Fig. 3 FTIR spectra (a) and Raman spectra (b) of GO and RGO reduced by different reductan

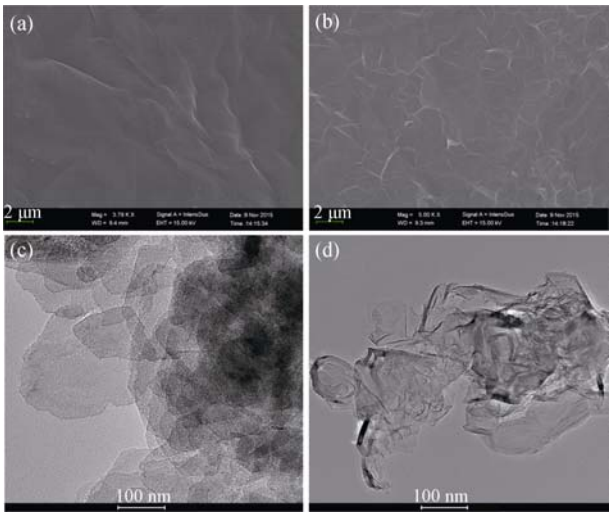

Fig. 4　SEM images of GO (a, b) and TEM images of RGO (c, d) reduced with $FeI_2/Ni(NO_3)_2$

Ni^{2+}. As stated by literature, Fe^{3+} which inhibits GO converting to RGO widely consists two features[24]: (a) the reaction temperature (95℃) is due to the promotion of the hydrolysis with exothermic reaction, which implies that the Fe^{2+} (strong Lewis acid) is decreased with the Fe^{3+}oppositely increased (b) Fe^{3+} hydrolysis is a multi-step and complex process, involving many reactions and intermediate products. Because of the decreased coordination ability of the hydrolysis product ($FeOH^{2+}$, $Fe(OH)^{2+}$) compared with Fe^{3+} (the catalytic capacity is also lessened), FeI_2 solutions are favorable for eliminating the reduction ability of carbon-oxygen. As a result, the bulk conductivity of RGO with $FeI_2/Ni(NO_3)_2$ is higher than that of RGO with FeI_2, where $Ni(NO_3)_2$ was introduced to inhibit the hydrolysis for the increased Lewis acids (Fe^{2+}).

$$Fe^{2+}–e^{-}=Fe^{3+} \qquad E^{\theta}=–0.771 \qquad (1)$$

$$Ni^{2+}–2e^{-}=Ni^{4+} \qquad E^{\theta}=–1.678 \qquad (2)$$

2.3　Electrochemical properties of RGO

As one of the most important parts in DSC, the counter electrode (Pt) acts as a catalyst by reducing the redox species (I^-/I_3^-), and thus regenerate the dye molecules. To real the CV results for RGO reduced with different reductants ize this function, counter electrode materials should possess superior catalytic activity in the DSC[29]. Figure 7(a) shows and platinized on FTO glass. Here, redox peakspacing (E_P)represents the catalytic capacity of materials. It can be seen that the RGO reduced by different reductants, exhibits its high catalytic performance (E_P(Pt) =0.55 V, E_P(FeI_2) = 0.50 V, E_P ($FeI_2/Ni(NO_3)_2$) = 0.35 V), when serving as counter electrode, implying that the highly catalytic RGO could be proposed to replace Pt in solar cells. Moreover, the RGO reduced by FeI_2/Ni $(NO_3)_2$ shows higher cathodic current density compared with the RGO reduced by FeI_2, because of its higher electrical conductivity. To

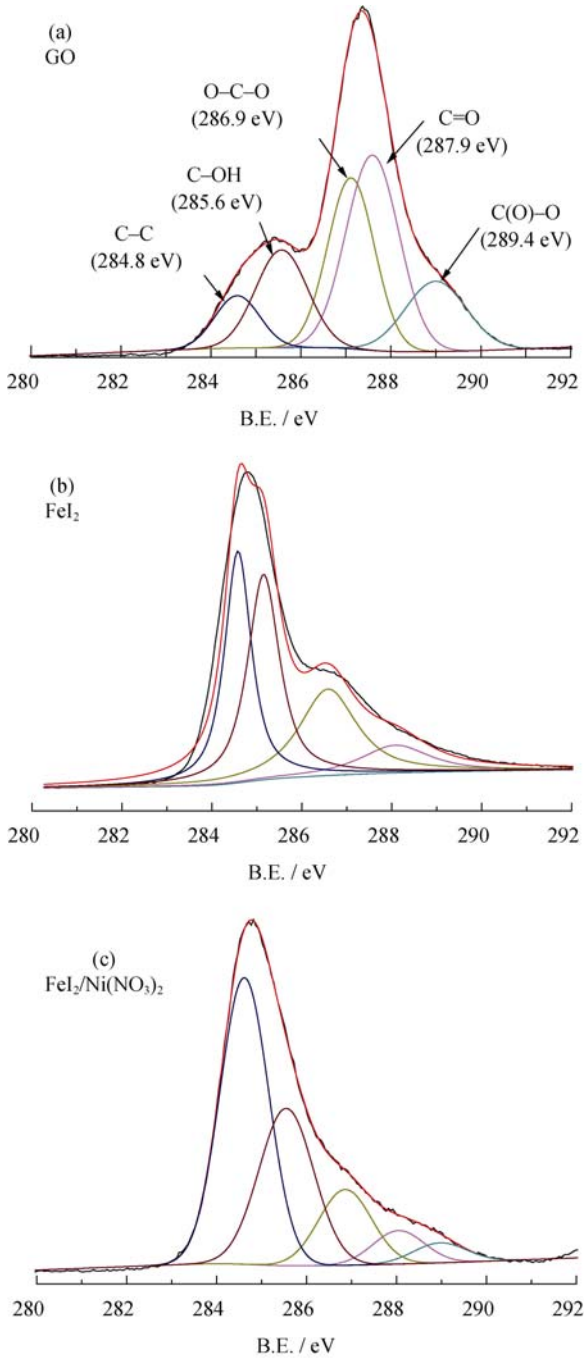

Fig. 5　XPS spectra of GO (a) and those of corresponding RGO reduced with FeI_2 (b) and $FeI_2/Ni(NO_3)_2$ (c)

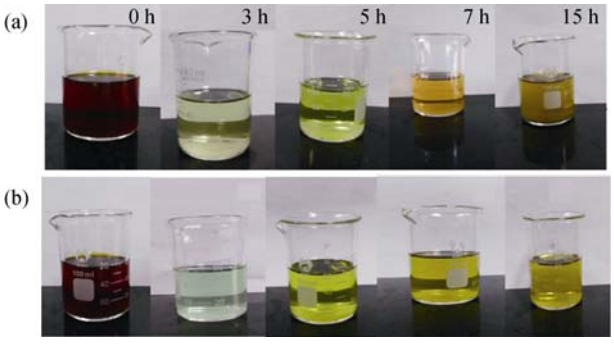

Fig. 6　Changes of color of different reductant with time
(a) FeI_2; (b) $FeI_2/Ni(NO_3)_2$

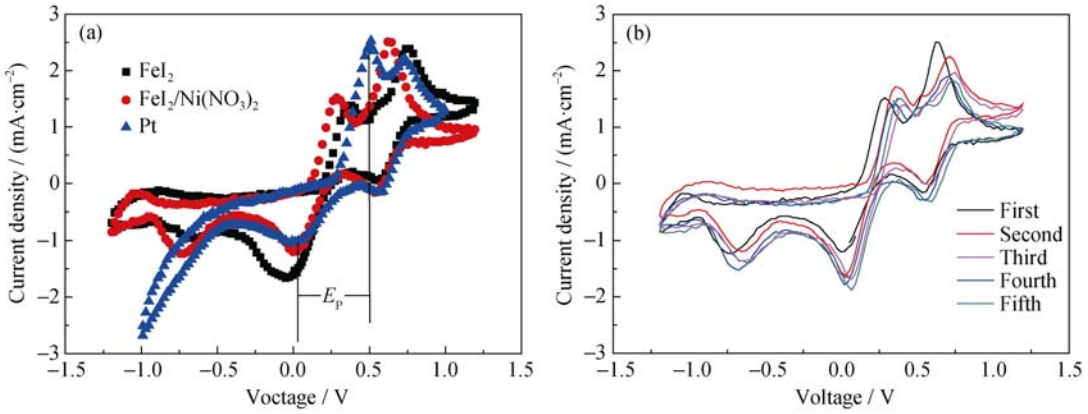

Fig. 7 CV curves for RGO reduced with different reductant (a) and CV curves for RGO reduced by FeI_2/ Ni$(NO_3)_2$ with different cycle numbers (b)

investigate the stability of the RGO reduced by FeI_2/ Ni $(NO_3)_2$ as electrode materials, the CV curves with different cycle numbers were studied (Fig. 7(b)). It shows that the cathodic current density decreases quite fast in the second cycle. With the cycle numbers increasing, the cathodic current density turns to be stable, which suggests the highly stable nature of the material and thus potential for long-term service which is critical for practical application.

3 Conclusion

We present an effective and environmentally friendly method to prepare RGO papers with high bulk conductivity of 30231 S/m. Ni$(NO_3)_2$ was adopted to inhibite the hydrolysis of strong Lewis acids (Fe^{2+}) in the preparation of RGO. The free-standing RGO papers serving as counter electrode showed high electrochemical activity. The work may shed light on providing a potentially low-cost, scalable, green, and effective route for large-scale production of graphene in future.

References:

[1] ROY-MAYHEW J D, BOZYM D J, PUNCKT C, *et al.* Functionalized graphene as a catalytic counter electrode in dye-sensitized solar cells. *ACS Nano*, 2010, **4(10):** 6203–6211.

[2] HU Y H, WANG H, HU B. Thinnest two-dimensional nano material-graphene for solar energy. *Chemsuschem*, 2010, **3(7):** 782–796.

[3] XU Z W, LI H J, CAO G X, *et al.* Synthesis of hybrid graphene carbon-coated nanocatalysts. *J. Mater. Chem.*, 2010, **20(38):** 8230–8232.

[4] VIET H P, TRAN V C, HUR S H, *et al.* Chemical fictionalization of graphene sheets by solvothermal reduction of a graphene oxide suspension in nmethyl-2-pyrrolidone. *J. Mater. Chem.*, 2011, **21(10):** 3371–3377.

[5] ZHOU X F, WANG F, ZHU Y M, *et al.* Graphene modified $LiFePO_4$ cathode materials for high power lithium ion batteries. *J. Mater. Chem.,* 2011, **21(10):** 3353–3358.

[6] HIRALAL P, IMAIZUMI S, UNALAN H E, *et al.* Nanomaterial enhanced all-solid flexible zinc-carbon batteries. *ACS Nano*, 2010, 4**(5):** 2730–2734.

[7] SU F Y, YOU C H, HE YB, *et al.* Pore diameter control in anodic titanium and aluminums oxides. *J. Mater. Chem.,* 2010, **20(2):** 9644–9650.

[8] ZHAO X, TIAN H, ZHU M Y, *et al.* Carbon nanosheets as the electrode material in superapacitors. *J. Power Sources*, 2009, **194(2):** 1208–1212.

[9] BAE J, SONG M K, PARK Y J, *et al.* Fiber super capacitors made of nanowire-fiber hybrid structures for wearable/flexible energy storage. *Angew Chem. Int. Edit*, 2011, **50(7):** 1683–1687.

[10] LI Z P, WANG J Q, LIU X H, *et al.* Electro static layer-by-layer self-assembly multilayer films based on graphene and manganese dioxide sheets as novel electrode materials for super capacitors. *J. Mater. Chem.*, 2011, **21(10):** 3397–3403.

[11] GAO Y J, MA D, WANG C L, *et al.* Reduced graphene oxide as a catalyst for hydrogenation of nitrobenzene at room temperature. *Chem. Commun.,* 2011, **47(8):** 2432–2434.

[12] MOHANTY N, NAGARAJA A, ARMESTO J, *et al.* High-through put ultrafast synthesis of solution-dispersed graphene *via* facile hydride chemistry. *Small*, 2010, **6:** 226–231.

[13] ZHANG H, LI Y, WANG Y, *et al.*P25-graphene composite as a high performance photocatalyst. *ACS Nano*, 2010, **4:** 380−386.

[14] LI Q, GUO B, YU J, *et al.* Highly efficient visible-light-driven photo catalytic hydrogen production of CdS-cluster-decorated grapheme nanosheets. *J. Am. Chem. Soc.*, 2011, **133:** 10878−10884.

[15] XIANG Q, YU J, JARONIEC M. Graphene-based semiconductor photo catalysts. *Chem. Soc. Rev.*, 2012, **41:** 782−796.

[16] ZHAO X C, LIN H, LI J F, *et al.* Low-cost preparation of a conductive and catalytic grapheme film from chemical reduction with AlI_3. *Carbon*, 2012, **50:** 3497–3502.

[17] KIM K S, ZHAO Y, JANG H, *et al.* Large-scale pattern growth of graphene films for stretchable transparent electrodes. *Nature*, 2009, **457(7230):** 706–710.

[18] SHEN J H, ZHU Y H, CHEN C, *et al.* Facile preparation and up conversion luminescence of graphene quantum dots. *Chem. Common.*, 2011, **47(9):** 2580–2582.

[19] JIANG B J, TIAN C G, WANG L, *et al.* Facile fabrication of high quality graphene from expands able graphite: simultaneous exfoliation and reduction. *Chem. Common.*, 2010, **46(27):** 4920–4922.

[20] ZUBAREV D Y, YOU X Q, CLEAN J, *et al.* Patterns of local aromaticity in grapheme ox radicals. *J. Mater. Chem.*, 2011, **21(10):** 3404–3409.

[21] DREYER D R, MURALI S, ZHU Y W, *et al.* Reduction of graphite oxide using alcohols. *J. Mater. Chem.*, 2011, **21(10):** 3443–3447.

[22] HE F A, FAN J T, MA D, *et al.* The attachment of Fe_3O_4 nanoparticles to graphene oxide by covalent bonding. *Carbon*, 2010, **48(11):** 3139–3144.

[23] PEI S F, ZHAO J P, DU J H, *et al.* Direct reduction of graphene oxide films into highly conductive and flexible grapheme films by hydrohalicacids. *Carbon*, 2010, **48(15):** 4466–4474.

[24] LIU C Y, HAO F, ZHAO X C, *et al.* Low temperature reduction of free-standing graphene oxide papers with metal iodides for ultra-high bulk conductivity. *Scientific Reports*, 2014, **4:** 3965.

[25] SHEN J F, YAN B, SHI M, *et al.* One step hydrothermal synthesis of TiO_2-reduced graphene oxide sheets. *J. Mater. Chem.*, 2011, **21(10):** 3415–3421.

[26] BAGRI A, MATTEVI C, ACIK M, *et al.* Structural evolution during the reduction of chemically derived graphene oxide. *Nat. Chem.*, 2010, **2(7):** 581–587.

[27] CANCADO L G, JORIO A, FERREIRA E H, *et al.* Quantizing defects in graphene *via* Raman spectroscopy at different excitation energies. *Nano Letters*, 2011, **11(8):** 3190–3196.

[28] PANSARE S V, PAUL E K. Organ catalytic symmetric direct vinylogous aldo lreactions of gamma-crotonolactone with aromatic aldehydes. *ChemCommun*, 2011, **47(3):** 1027–1029.

[29] SAITO Y, KUBO W, KITAMURA T, *et al.* I^-/I_3^- (-) redox reaction behavioronpoly (3, 4-Ethylenedioxythiophene) counter electrode in dye-sensitized solar cells. *J. Photochem. Photobio. A*, 2004, **164(3):** 153–157.

基于 FeI_2/Ni^{2+}溶液还原制备低成本的高导电性及催化性纸张石墨烯

南 辉[1], 王文利[2], 韩建华[1], 尹学文[1], 周 宇[1], 赵晓冲[3], 林 红[1]

(1. 清华大学 材料学院, 新型陶瓷与精细工艺国家重点实验室, 北京 100084; 2. 苏州大学 纺织与服装工程学院, 苏州 215123; 3. 中国工程物理研究院 材料研究所, 绵阳 621907)

摘 要: 采用基于 FeI_2/ $Ni(NO_3)_2$ 溶液的温和化学法还原制备低成本的纸张型石墨烯, 并对其导电与催化性能进行了研究。研究结果表明: 在 pH=1.5, 温度为 95℃的条件下处理 6 h, 得到电导率高达 30231 S/m 的纸张型石墨烯, 这是由于作为强路易斯酸的 Fe^{2+}促进了亲核取代反应, 提高了还原效率, 从而提高了纸张型石墨烯的电导率; 而 Ni^{2+}通过减少溶液中的 H^+来抑制 Fe^{2+}的水解, 从而保证 Fe^{2+}对石墨烯的充分还原以及达到保护环境的目的。此外, 基于此还原工艺制备的纸张型石墨烯在 I^-/I^{3-}电解液中可以获得接近铂电极的电流密度, 表明制备出的纸张型石墨烯具有较好的催化性能，并可以为电子提供快速的传出通道, 使其在太阳能电池中表现出较好的应用前景。

关 键 词: 石墨烯; 金属离子; 化学还原; 电导率; 催化

中图分类号: TQ174 **文献标识码:** A